JOURNAL OF COMPUTATIONAL PHYSICS 79, 270–297 (1988)

Moving Finite Element Methods for Evolutionary Problems. II. Applications

I. W. JOHNSON

Department of Mathematics, University of Reading, England

A. J. WATHEN

School of Mathematics, University of Bristol, England

M. J. BAINES

Department of Mathematics, University of Reading, England

Received October 13, 1986; revised September 1, 1987

In this, the second of two papers on the subject, we present applications of the moving finite element method to a number of test problems. Key features are linear elements, a direct approach to parallelism and node overtaking (avoiding penalty functions), rapid inversion of the mass matrix by preconditioned conjugate gradients, and explicit Euler time stepping. The resulting codes are fast and efficient and are able to follow fronts and similar features with great accuracy. The paper includes a substantial section on changes of dependent variable and front tracking techniques for non-linear diffusion problems. Test problems include non-linear hyperbolic conservation laws and non-linear parabolic equations in one and two dimensions.

1. INTRODUCTION

In Baines and Wathen [1], hereafter called Part I, it was shown that in one dimension the moving finite element (MFE) method, invented by Miller [2], is (without penalty functions) a purely local method, being also a special case of a class of fixed and moving finite element methods for evolutionary problems based on local elementwise projections. It was also shown in Part I that the corresponding method in higher dimensions is a particular (global) projection of the local method, as is the fixed finite element (FFE) Galerkin method in any number of dimensions. The current paper gives examples of practical calculations using the method of Part I in one and two dimensions. Both hyperbolic and parabolic problems are included, while for parabolic problems a discussion of some technical aspects of the approximation and of the choice of dependent variable is also given. Some examples on systems of equations are also presented.

Applications of the MFE method have appeared in several recent papers (Gelinas, Doss and Miller [3], Dukowicz [4], Mosher [5], Hrymak *et al.* [6]).

0021-9991/88 $3.00

These employ a direct global application of the technique and also incorporate penalty functions to overcome parallelism (q.v.) and node overtaking. Implicit methods and a stiff solver are used to time step the semi-discrete MFE equations.

The approach adopted here differs from these in that penalty functions are avoided, simple projections are used and the time stepping is explicit Euler. The consistent mass matrix is shown to be well conditioned when diagonally preconditioned and, as a result, is inverted rapidly using preconditioned conjugate gradients [7]. As a result, the method is much faster and, although special techniques are still required to avoid singularities, these are direct (see below). In the present paper we present a number of examples using this approach.

Scalar hyperbolic problems are discussed in Section 2 together with shock modelling techniques: most of the theory has already appeared in Part I, Section 4, however. Section 3 is a substantial section in which problems involving parabolic terms (linear and non-linear) are discussed from the present point of view. As in the papers cited above, special treatment of second derivative terms is necessary, and this is discussed in Section 3 together with some useful ideas on transformation of the dependent variable. Examples are given in both one and two dimensions.

In Section 4 the approach is applied to hyperbolic systems of equations and a discussion given of the advantages and of the difficulties involved. Finally in Section 5 we consider some open questions concerning MFE type methods.

First, however, we discuss two issues common to all these MFE applications, namely parallelism (or collinear/coplanar nodes), the presence of which causes singularity of the mass matrix, and node overtaking. A full discussion is given in Wathen and Baines [8] but we summarise the problems and their direct cures here.

Parallelism arises from the loss of rank of the matrix A of Part I, Section 2. This is due to the fact that two or more test functions become coincident when the slopes of the solution in adjacent elements become equal. A simple remedy is to omit the particular MFE equation corresponding to the superfluous test functions, leaving an underdetermined system. A particular solution of this system is easily obtained (by, for example, setting the speeds of the parallel nodes equal to zero) (see Wathen and Baines [8]). Then, by adding a suitable multiple of the appropriate (very simple) null space, these zero nodal speeds may be adjusted to any desired (e.g., averaged) value. This is the procedure used in the calculations done here.

The second issue concerns the time-stepping method used to fully discretise each problem. The MFE method itself is non-linear (see Part I) (even for linear problems) and thus any implicit method will require the solution of systems of non-linear equations. Gelinas, Doss, and Miller [3] have computed solutions to a large number of problems using implicit methods. Our approach is, on the contrary, to use the simplest possible explicit method, namely the forward Euler method, in all our computations. This has allowed considerable flexibility in dealing with the different classes of problems we have considered.

In particular, we can determine in advance the time steps which give rise to node overtaking. This allows us to choose sufficiently small time steps to avoid this difficulty. In this sense the time step restriction is a kind of stability condition.

However, in hyperbolic problems such as those discussed in Sections 2 and 4 below, we deliberately allow node overtaking in order to imitate shock formation.

Various strategies for time stepping in all problems have been devised to encourage smooth nodal movement. Such restrictions are associated with accuracy considerations which, apart from simple truncation error analysis, still suffer from the lack of a formal analysis (but see Dupont [9]).

One such time stepping strategy, due to Please [10], is to restrict the slope of the solution to change only by a small proportion. The other, due to Sweby [11], is to restrict the relative motion of nodes to be monotonic (i.e. that the distance between them does not pass through a turning point). These are designed for use in non-shock problems.

We move now to the first set of examples, those for scalar hyperbolic problems.

2. Scalar Hyperbolic Problems

In this section we give illustrations of the use of the MFE method in solving scalar hyperbolic equations of the form

$$u_t + \nabla \cdot \mathbf{f} = 0, \tag{2.1}$$

in both one and two dimensions.

2.1. *One-dimensional Problems*

The first example is the equation

$$u_t + uu_x = 0 \tag{2.2}$$

with piecewise linear initial data, as in Fig. 2.1. In this, the simplest non-linear scalar equation, a number of special situations in MFE occur. With a continuous piecewise linear approximation U to u, the operator $L(U) = -UU_x$ is piecewise linear in each element although discontinuous between elements in general. It therefore lies in S_ϕ without further projection (see Part I, Section 2) but, moreover, it also happens to lie in $S_{\alpha\beta}$. Thus the $\dot{w}_k$ of Part I, Eq. (2.7), is immediate and so is the $\dot{\mathbf{y}}$ of Part I, Eq. (3.14). As a result, for the element k,

$$\dot{w}_k = \begin{pmatrix} -m_k a_{j-1} \\ -m_k a_j \end{pmatrix} \tag{2.3}$$

(cf. Section 4 of Part I) and, for the node j,

$$\begin{aligned} \dot{a}_j &= 0 \\ \dot{s}_j &= a_j. \end{aligned} \tag{2.4}$$

In this case the MFE equations are identical with the equations for the solution of (2.2) by characteristics.

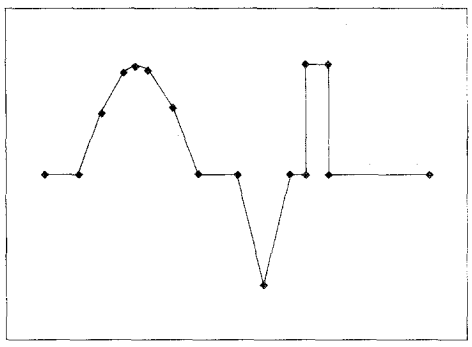

FIG. 2.1. Initial data for the MFE solution of Bergers' equation in one dimension.

Furthermore, the integration of (2.4) is trivial and there is no error in forward Euler time stepping. For Eq. (2.2) therefore the MFE method described in Part I, Section 4 is exact, at least until shocks occur. Shock formation may be associated with node overtaking in the sense that, as a segment of the solution overturns, a shock is detected (see Section 4.6 of Part I). When this occurs the vertical segment may be constrained to remain vertical while the horizontal speed of its midpoint is maintained. The result is a two-point representation of a shock with the correct shock speed as calculated from the jump condition. The identification of the MFE method with the solution by characteristics and the consistency of the element motions with the local wave speeds ensures entropy satisfaction. This is also true for scalar expansion waves: for example, a vertical segment will expand with the correct spread, corresponding to the similarity solution. Shock merging may be treated in a similar way to shocks.

We illustrate these features by taking the initial data in Fig. 2.1 and running it through shock formation to a time when the character of the final solution is evident (Fig. 2.2).

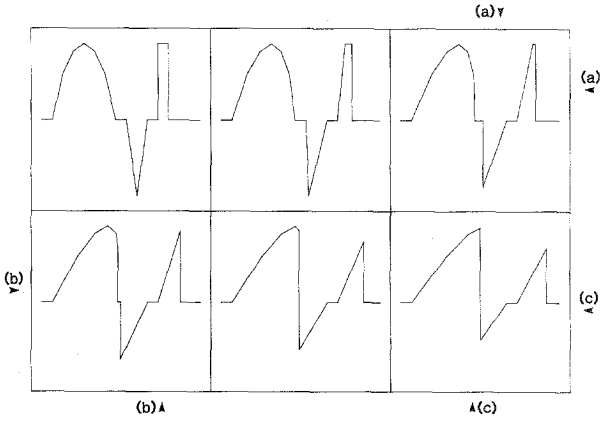

FIG. 2.2. MFE solution of Burgers' equation at time (a) $t = 0.5$; (b) $t = 1.0$; (c) $t = 1.5$.

The second example chosen is the Buckley–Leverett equation

$$u_t + f(u)_x = 0 \tag{2.5}$$

with the non-convex flux function

$$f(u) = \frac{u^2}{u^2 + (1/2)(1-u)^2} \tag{2.6}$$

as in, e.g., Concus and Proskurowski [12]. In this case, $-f(U)_x$ must be projected into S_ϕ, and there will be a projection error not present in the previous example. Taking a piecewise linear approximation U as before, we project $L(U)$ into the local element space S_ϕ as in Part I, Section 4.1. This gives $\dot{\mathbf{w}}_k$ and the local segment motions of Part I, Section 4.2. Transfer of this information on to the node j leads to ordinary differential equations (ODEs) of the form of Part I, Eq. (4.13) for the $\dot{a}_j$ and $\dot{s}_j$. We use Euler forward differences to step these ODEs forward in time, giving rise to an evolution error. Unlike the previous example, the time step must be chosen small enough to give a required accuracy. The "shock" or discontinuity when it appears is modelled as before, by freezing the angular speed of the overturning segment and continuing the midpoint speed smoothly.

The initial data

$$U \sim u = 0.1/(0.1 + x) \tag{2.7}$$

and the MFE solution at subsequent (even) time steps are shown in Fig. 2.3. Time steps were taken to be 0.1 here.

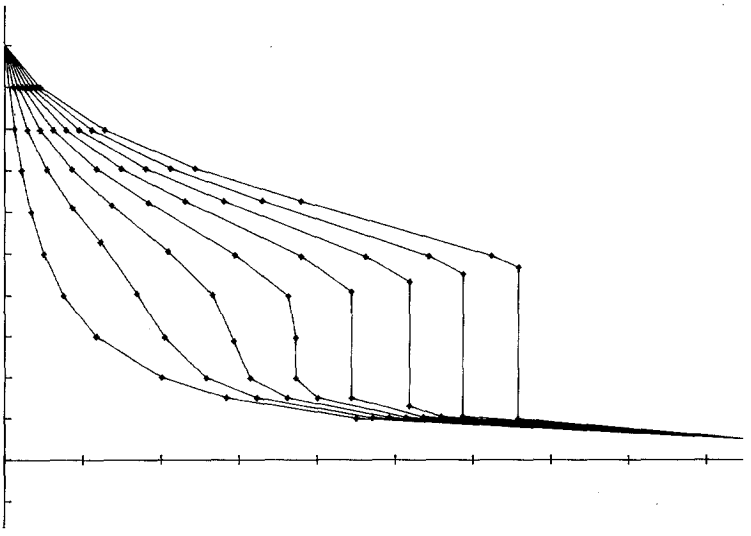

FIG. 2.3. Initial data and MFE solution of one-dimensional Buckley–Leverett equation.

2.2. *Scalar Hyperbolic Problems in 2-dimensions*

In Part I it was shown that the MFE method in two and higher space dimensions is non-local, but that a closely related local method exists (Section 5.3 of Part I). We give here the results of two computations on the same problem, one with the local and one with the non-local method.

The problem is a simplification of the porous media flow of incompressible immiscible fluids when the total flow is specified. (The details of the derivation of the model are given in [13]).

The appropriate differential equation is

$$\frac{\partial u}{\partial t} + \nabla \cdot \frac{u^2}{u^2 + (3/4)(1-u)^2} = 0 \tag{2.8}$$

on a square region $(x, y) \in [0, 4]^2$ with $u(0, 0, t) = 1$ and $\partial u/\partial \eta = 0$ on the boundary. The initial condition is

$$u(x, y, 0) = \frac{0.1}{0.1 + (1/4)\sqrt{x^2 + y^2}} \tag{2.9}$$

and is represented by simple nodal interpolation on an unsophisticated regular mesh (Fig. 2.4). An isometric plot of the discrete initial data is also shown in Fig. 2.4. The approximate solution after 24 explicit Euler time steps of length $\Delta t = 0.025$ is given in Fig. 2.5a for the non-local MFE method and in Fig. 2.5b for the related local method. In each case nodes at the corners of the region are held fixed, while other nodes on the boundaries are free to move only along the boundary. The solution discontinuity shown in the figures forms between time steps 17–18 in each computation. Subsequently the node points of a folded triangular element are constrained to move normal to the line of the folded element at the Hugoniot shock speed. The details are given in [8, 13].

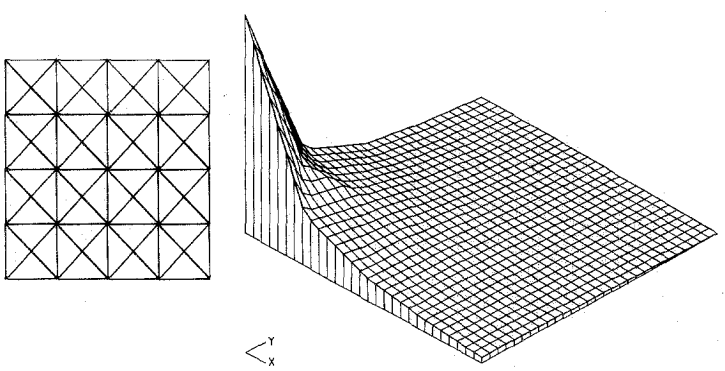

Fig. 2.4. Initial mesh and data for MFE solution of the two-dimensional generalisation of the Buckley–Leverett equation.

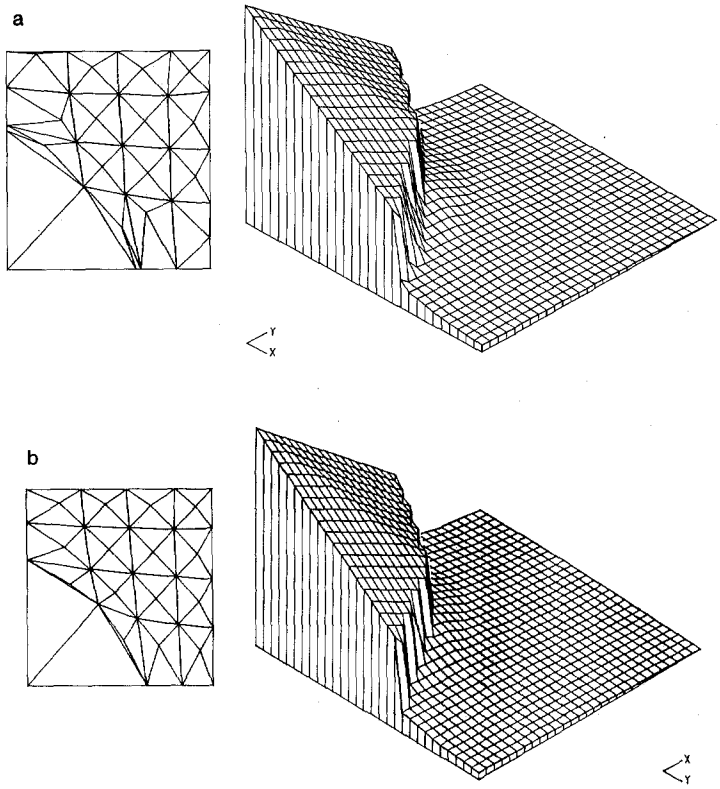

FIG. 2.5. (a) Global MFE solution of two-dimensional Buckley–Leverett equation after 24 explicit steps of length 0.025. (b) Local MFE solution of two-dimensional Buckley–Leverett equation after 24 explicit steps of length 0.025.

This approach ignores any sideways movement of the shock. However, consideration of segment motions of triangular elements in 2-dimensions is expected to afford a more precise description of the problem of a curved moving shock. This is the subject of present research, although the essential ideas appear in [14].

3. PARABOLIC PROBLEMS

In this section we describe the application of MFE to a number of parabolic problems whose solutions exhibit steep moving fronts. Before doing so we discuss in detail some smoothing procedures which are necessary to interpret inner products involving second-order operators which appear in the MFE formulation (cf. Part I, Section 5.1).

3.1. *Second-Order Operators*

As in Part I we consider evolution equations of the form

$$u_t = L(u), \tag{3.1}$$

where L is a second-order spatial differential operator, and seek an approximate finite element solution in the form

$$U = \sum a_j \alpha_j \tag{3.2}$$

with piecewise linear basis functions α_j as in Part I, Section 1.

In the analysis of Part I it was generally assumed that U lies in the domain space of the spatial operator L, but for parabolic problems L will contain second order terms (e.g., $L(u) = u_{xx}$) and in this case $L(U)$ exists only in the sense of distributions and has infinite L_2 norm. As in Part I, we define a suitable smoothing operator S which is such that $S(U)$ has sufficient continuity to lie in the domain space of L, and the projection of $L(U)$ into the space $S_{\alpha\beta}$ is interpreted as

$$\lim_{S \to I} PL(S(U)), \tag{3.3}$$

where I is the identity operator (cf. Part I, Eq. (5.1)).

In the finite element approach the Galerkin equations are derived by formally minimising

$$\| U_t - L(U) \|_{L_2}^2 \tag{3.4}$$

(cf. Part I, Eq. (3.7)).

In the fixed finite element (FFE) method, the resulting Galerkin equations involve evaluation of the inner products

$$\langle L(U), \alpha_i \rangle, \tag{3.5}$$

where $\langle \cdot, \cdot \rangle$ denotes the standard L_2 inner product. If L contains second or higher order derivatives, (3.4) should formally be replaced by

$$\| U_t - L(S(U)) \|_{L_2}^2, \tag{3.6}$$

so that $L(S(U))$ has finite L_2 norm, and (3.5) correspondingly replaced by

$$\langle L(S(U)), \alpha_i \rangle. \tag{3.7}$$

Little attention is paid to the smoothing operator S in the FE case, since (3.5) exists and is readily evaluated using integration by parts.

For an MFE solution of (3.1) with both the coefficients a_j and basis functions α_j

dependent on time (cf. Miller [2]) the MFE equations are derived by minimising (3.4) with respect to the parameters $\dot{a}_j$ *and* the nodal velocities $\dot{s}_j$, leading to Galerkin equations which require evaluation of the inner products

$$\langle L(U), \alpha_i \rangle \tag{3.8}$$

and

$$\langle L(U), \beta_{ji} \rangle, \qquad j = 1, ..., d, \tag{3.9}$$

where d is the number of space dimensions. The additional basis functions β_{ji} may be written as a vector $\boldsymbol{\beta}_i$ defined by

$$\boldsymbol{\beta}_i = -(\nabla U)\, \alpha_i \tag{3.10}$$

(cf. Part I, Eqs. (1.13) and (1.14)).

The inner products (3.8) may be evaluated using integration by parts as in the fixed finite element method, but since the components of the $\boldsymbol{\beta}_i$ are discontinuous at the nodes and across element boundaries (see Part I, Fig. 1.1), (3.9) does not exist. We must replace (3.9) by

$$\langle L(S(U)), \boldsymbol{\beta}_i \rangle \tag{3.11}$$

and address the problem of defining the smoothing operator S in order to evaluate (3.11). In the discussion of smoothing procedures which follows attention shall be focused on the simplest one-dimensional case

$$L(U) = U_{xx} \tag{3.12}$$

but extensions to more general operators and higher dimensions will be indicated as appropriate. With L defined by (3.12) we require to define a smoothing operator S such that the inner product

exists.

In his original formulation of the MFE method Miller [1] defines $S(U)$ as

$$S(U)(x) = \int_{-\infty}^{\infty} \rho^{\delta}(x-y)\, U(y)\, dy, \tag{3.14}$$

where ρ^{δ} is a C_0^{∞} function of unit total integral which has support within an interval of radius δ about the origin. This process is known as "δ-mollification" and may be interpreted as replacing the original basis functions α_i in (3.2) by "mollified" basis

functions α_j^δ which have sufficient continuity to ensure that (3.13) exists in the limit as $\delta \to 0$. Evaluating (3.13) with $S(U)$ defined by (3.14) yields

$$\langle U_{xx}, \beta_i \rangle \to -\tfrac{1}{2}(m_{i+1}^2 - m_i^2), \tag{3.15}$$

where

$$m_i = \frac{\Delta a_i}{\Delta s_i} = \frac{a_i - a_{i-1}}{s_i - s_{i-1}},$$

independent of the smoothing δ as $\delta \to 0$. Extension of this technique to more general operators and to higher dimensions may be achieved [30].

In their variational formulation of MFE, Mueller and Carey [15] interpret inner products involving second order operators by assuming an arbitrary smoothing, such that $\nabla(S(U))$ is continuous across element boundaries so that Green's theorem may be applied. This procedure yields the same result (3.15) as δ-mollification for the inner products (3.13) but since the approach generalises to non-linear operators we shall describe the interpretation of

$$\left\langle \frac{\partial}{\partial x}(D(U)\, U_x), \beta_i \right\rangle \tag{3.16}$$

for a general function $D(U)$.

Recalling the definition (3.10) of β_i, (3.16) may be expressed as

$$\left\langle \frac{\partial}{\partial x}(D(U)\, U_x), -U_x \alpha_i \right\rangle = -\int_{s_{i-1}}^{s_{i+1}} \frac{\partial}{\partial x}(D(U)\, U_x)\, U_x \alpha_i \, dx. \tag{3.17}$$

The integral (3.17) may be rewritten using Green's theorem, as

$$-\int_{s_{i-1}}^{s_{i+1}} \frac{\partial}{\partial x}(\alpha_i U_x D(U)\, U_x)\, dx + \int_{s_{i-1}}^{s_{i+1}} \frac{\partial}{\partial x}(\alpha_i\, U_x)\, D(U)\, U_x dx. \tag{3.18}$$

Assuming an arbitrary smoothing such that U_x is continuous at node s_i, the first term in (3.18) vanishes and the second term may be expanded to give

$$\int_{s_{i-1}}^{s_{i+1}} D(U)\, U_x U_x (\alpha_i)_x \, dx + \int_{s_{i-1}}^{s_{i+1}} D(U)\, \alpha_i \frac{\partial}{\partial x}(\tfrac{1}{2} U_x^2)\, dx. \tag{3.19}$$

Using Green's theorem again, the second term in (3.19) may be written

$$\int_{s_{i-1}}^{s_{i+1}} \frac{\partial}{\partial x}(D(U)\, \alpha_i\, \tfrac{1}{2} U_x^2)\, dx - \int_{s_{i-1}}^{s_{i+1}} (D(U)\, \alpha_i)_x\, \tfrac{1}{2} U_x^2\, dx \tag{3.20}$$

and, assuming continuity of U_x at s_i once more, the first term in (3.20) vanishes yielding the resulting expression for (3.16) as

$$\left\langle \frac{\partial}{\partial x}(D(U)\,U_x), \beta_i \right\rangle = \int_{s_{i-1}}^{s_{i+1}} (D(U)\,U_x^2(\alpha_i)_x - \tfrac{1}{2}(D(U)\,\alpha_i)_x U_x^2)\,dx \qquad (3.21)$$

which is equivalent to (3.15) in the case $D(U)=1$.

A similar analysis may be used in two space dimensions [24], assuming an arbitrary smoothing of the gradients U_x, U_y across element edges to give the corresponding result

$$\langle \nabla\cdot(D(U)\,\nabla U), \boldsymbol{\beta}_i\rangle = \int_{\Omega_i} (D(U)\,\nabla U(\nabla U\cdot\nabla\alpha_i) - \tfrac{1}{2}\nabla(D(U)\,\alpha_i)\,\nabla U\cdot\nabla U)\,d\Omega_i$$
$$+ \text{boundary terms if node } i \text{ is on the boundary,} \qquad (3.22)$$

where Ω_i is the patch of elements around node i over which α_i has support and $\boldsymbol{\beta}_i$ is as in Part I, Eq. (1.8).

For one-dimensional problems we have used an approach suggested by Morton [16] (see [17] for details) in which the smoothing operator S is defined explicitly as

$$S(U)(x) = w(x) \qquad (3.23)$$

by constructing a "recovered" function $w(x)$ from the piecewise linear approximation $U(x)$ (or its gradient $U_x(x)$) which has sufficient continuity to allow evaluation of the inner products (3.11). Suitable functions $w(x)$ may be constructed by fitting local polynomials of sufficiently high order to $U(x)$ or $U_x(x)$.

If the recovered function $w(x)$ is defined on the element connecting nodes i an $i-1$ by the Hermite cubic function satisfying

$$\begin{aligned} w(s_{i-1}) &= U_{i-1}, & w(s_{i-1}) &= \tfrac{1}{2}(m_i + m_{i-1}) \\ w(s_i) &= U_i, & w(s_i) &= \tfrac{1}{2}(m_i + m_{i+1}), \end{aligned} \qquad (3.23)$$

then

$$\langle w_{xx}, \beta_i\rangle = -\tfrac{1}{2}(m_{i+1}^2 - m_i^2),$$

which is entirely equivalent to using δ-mollification or to assuming an arbitrary smoothing of U_x. Also

$$\langle w_{xx}, \alpha_i\rangle = m_{i+1} - m_i,$$

consistent with standard integration by parts. Hence we have shown that the recovery procedure encompasses the smoothing procedures described above. Since we may define $w(x)$ in a variety of different ways the recovery procedure offers greater flexibility than the other methods described with no loss of computational

efficiency in one dimension. Numerical experiments suggest that improved accuracy and less restrictive time steps are afforded by exploiting superconvergence ideas and fitting a quadratic function $w_x(x)$ to the MFE gradient U_x, defined on the element between nodes i and $i-1$ by

$$\begin{aligned} w_x(s_{i-1}) &= (1-\theta)\, m_{i-1} + \theta m_i \\ w_x(\tfrac{1}{2}(s_i + s_{i-1})) &= m_i \\ w_x(s_i) &= \varphi m_i + (1-\varphi)\, m_{i+1} \end{aligned} \tag{3.24}$$

where

$$\theta = \frac{\Delta s_i}{\Delta s_i + \Delta s_{i-1}} \quad \text{and} \quad \varphi = \frac{\Delta s_i}{\Delta s_i + \Delta_{s_{i+1}}}$$

(see Johnson [17]). This form of recovery is used in the one-dimensional numerical results given later in this section.

The recovery technique may be used for more general operators and has been implemented successfully on a linear problem in two dimensions. In two dimensions the construction of a recovered function over an element requires information from the solution in the surrounding elements so that a strictly elementwise assembly of inner products is no longer possible and consequently efficiency is reduced. Although we have found from our experience using MFE in one dimension that recovery techniques can improve accuracy and allow larger time steps, the substantial increase in computational effort involved in using recovery in two dimensions has led us to choose the more compact form (3.22) to evaluate element inner products in this case. In particular, cases where high accuracy is given greater priority than computational efficiency it may be appropriate to use recovery.

We shall now use the recovery procedure described above to give an analysis of nodal movement for the MFE solution of Burgers' equation in one dimension, together with numerical results for a particular test problem.

3.2. *MFE Solution of Burgers' Equation*

In this section we consider solution of the viscous Burgers' equation

$$u_t + uu_x = \varepsilon u_{xx} \tag{3.25}$$

which develops steep moving fronts in the case $\varepsilon \ll 1$.

3.2.1. *Analysis of Nodal Movement*

We seek a piecewise linear MFE solution $U(x, t)$ in the form (3.2) of

$$U_t + UU_x = \varepsilon U_{xx}. \tag{3.26}$$

Using the recovery technique described above, this is equivalent to solving

$$U_t + UU_x = \varepsilon w_{xx} \tag{3.27}$$

for a suitably defined recovered function $w(x)$ [17].

The time derivative in (3.26) is given by (cf. Part I, Eq. (1.9))

$$U_t = \sum \dot{a}_j \alpha_j + \dot{s}_j \beta_j \tag{3.28}$$

and the convection term may be expressed as

$$UU_x = -\sum a_j \beta_j \tag{3.29}$$

(cf. [13]).

If we define $w(x)$ by fitting a cubic to $U(x)$ (or a quadratic to $U_x(x)$) within an element, then $w_{xx}(x)$ is a piecewise linear discontinuous function and may thus be expressed as

$$w_{xx} = \sum c_j \alpha_j + b_j \beta_j \tag{3.30}$$

for suitable coeffiients c_j, b_j. Substituting (3.28), (3.29), (3.30) in (3.27) we have

$$\sum (\dot{a}_j \alpha_j + s_j \beta_j - a_j \beta_j) = \varepsilon \sum (c_j \alpha_j + b_j \beta_j). \tag{3.31}$$

Both sides of (3.31) lie in the space $S_{\alpha\beta}$ spanned by the $\{\alpha_i, \beta_i\}$, hence no projection is necessary, (cf. Part I, Section 1), and using the discontinuity of the functions β_i at the nodes we obtain the solution

$$\begin{aligned} \dot{a}_j &= \varepsilon c_j \\ \dot{s}_j &= a_j + \varepsilon b_j. \end{aligned} \tag{3.32}$$

It is now possible to see how the nodal velocities $\dot{s}_j$ are affected by the choice of coefficients b_j which appear in (3.30), i.e., by the choice of smoothing for the second-order operator. From (3.30) we have

$$b_j = \frac{(w_{xx})_{j+} - (w_{xx})_{j-}}{m_{j+1} - m_j}$$

and it may be seen that it is the jump in w_{xx} that drives the motion of the nodes, and hence that different choices of w may provide substantially different nodal

movement. In particular we note that if $w(x)$ is defined by fitting a cubic spline to $U(x)$, so that $w_{xx}(x)$ is continuous at the nodes, we have

$$b_j = 0 \qquad \text{for each } j$$

and hence from (3.32) the nodes will then always move as in the limiting hyperbolic case $\varepsilon = 0$.

In the next section we give numerical results using MFE for a particular example of (3.25) with the recovered function chosen as the quadratic defined by (3.24). The semi-discrete solution (3.32) is advanced using explicit Euler time stepping with a fixed time step which is chosen to be small enough to ensure that nodes do not overtake.

3.2.2. *Numerical Results*

A particular solution of

$$u_t + uu_x = \varepsilon u_{xx}, \qquad x \in [0, 1]$$

may be obtained using the Cole–Hopf transformation giving

$$u(x, t) = f(\xi),$$

where

$$\xi = x - \mu t - \beta$$

and

$$f(\xi) = \left[\mu + \alpha + (\mu - \alpha)\exp\left(\frac{\alpha\xi}{\varepsilon}\right)\right] \Big/ \left[1 + \exp\left(\frac{\alpha\xi}{\varepsilon}\right)\right], \tag{3.33}$$

where α, β, and μ are arbitrary constants. Initial and boundary conditions are obtained from (3.33) as

$$u(x, 0) = f(x - \beta)$$
$$u(0, t) = f(-\mu t - \beta)$$
$$u(1, t) = f(1 - \mu t - \beta)$$

and the values of the arbitrary constants were chosen as $\alpha = 0.4$, $\beta = 0.125$, $\mu = 0.6$.

be approximated to high accuracy by Dirichlet conditions

$$u(0, t) = 1 \cdot 0$$
$$u(1, t) = 0 \cdot 2.$$

Numerical results using MFE, as described above, with 8 moving nodes and $\Delta t = 1 \times 10^{-3}$ are compared with the analytic solution (3.33) in Fig. 3.1.

3.3. *MFE For Non-linear Diffusion Problems*

In this section we consider MFE solutions of non-linear diffusion equations of the type

$$u_t = \nabla \cdot (D(u) \nabla u) \tag{3.34}$$

for some general function $D(u)$. One case of particular interest is

$$D(u) = u^n \qquad (n > 0) \tag{3.35}$$

which describes many physical processes, e.g., seepage of a fluid in a porous medium, spreading of a thin viscous film under gravity and the propagation of radiation waves. Similarity solutions exist in this case and have been studied by Ames [18], Tayler, Ockenden, and Lacey [19], and Zel'dovich and Kompaneets [20] among others. Numerical solutions in the presence of an additional source term have been studied by Tomoeda [21], and for general $D(u)$ by Meek and Norbury [22]. Before we describe the MFE solution of (3.34) we shall introduce a change of dependent variable which has some very desirable features.

3.3.1. *Change of Dependent Variable*

The behaviour of solutions of (3.34) is of particular interest if there exist degenerate points at which $D(u) = 0$, in which case the coefficients on the RHS of (3.34) typically become unbounded. In the case (3.35) a degenerate point $u = 0$ represents a moving interface and from similarity solutions it may be seen that $\nabla^2 u$ is unbounded as $u \to 0$. Such points of degeneracy require careful attention in any

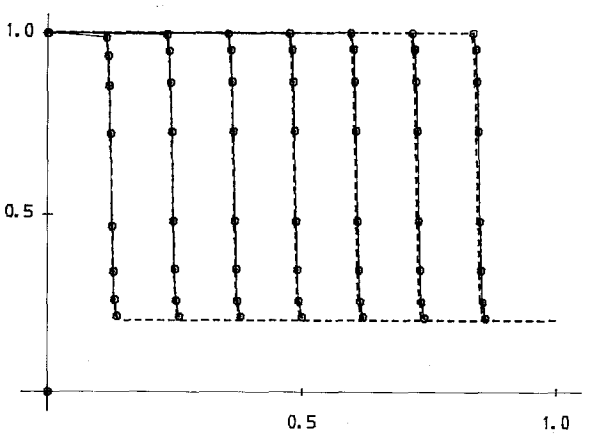

FIG. 3.1. Initial data, MFE and analytic solutions of the viscous Burgers' equation in one dimension, time $t = 0.0$ to $t = 1.2$.

numerical solution, but it may be possible to transform the problem in such a way that the coefficients in the transformed problem remain bounded at the points of degeneracy.

For numerical solution of problems of type (3.34) with $D(u)$ defined by (3.35), together with an additional source term, Tomoeda [21] suggests that this may be achieved by a change of dependent variable of the form

$$v = u^n. \tag{3.36}$$

Using this transformation in the equation

$$u_t = \nabla \cdot (u^n \nabla u) \tag{3.37}$$

yields

$$v_t = v\nabla^2 v + \frac{1}{n}(\nabla v)^2 \tag{3.38}$$

and for similarity solutions of (3.37) it may be verified that in the transformed problem both ∇v and $\nabla^2 v$ remain bounded as $v \to 0$. At the degenerate point $v = 0$, (3.38) reduces to the hyperbolic equation

$$v_t = \frac{1}{n}(\nabla v)^2. \tag{3.39}$$

Please and Sweby [23] have shown that the transformation (3.36) is a particular example of a class of transformations appropriate for general problems of type (3.34). For the numerical solution of these problems they suggest a transformation to a new dependent variable φ given by

$$\varphi = -\int_0^u \frac{D(p)}{p}\, dp \tag{3.40}$$

which transforms (3.34) to

$$\varphi_t = D(u)\nabla^2 \varphi - (\nabla \varphi)^2. \tag{3.41}$$

They also point out that if $\mathbf{w}$ is the velocity of a moving wave solution of (3.34) then the new variable φ represents the velocity potential, i.e., $\mathbf{w} = \nabla \varphi$.

Numerical results using MFE together with the transformation (3.40) for a problem in semi-conductor device modelling with a complicated functional form for $D(u)$ are given at the end of this section. It may be noted that with $D(u)$ defined by (3.35) the transformation defined by (3.40) is the same as that suggested by Tomoeda [21], up to a constant multiple. We shall now use the transformation to derive expressions for the velocity of a moving interface which provides a front tracking technique which is incorporated in the MFE solution.

3.3.2. *Front Tracking With MFE*

In any numerical solution of problems of type (3.37) it is advantageous that the moving interface $u=0$ should coincide with a mesh point in the discrete formulation. If a discrete approximation to the velocity of the interface point is available a moving mesh method such as MFE is particularly attractive since a mesh point located initially at the interface may be constrained to move with the interface velocity and hence remain at the interface (approximately) for all time. In this section we shall derive analytic expressions for the interface velocity in (3.37) by considering the transformed problem (3.38) which we shall discretize and incorporate as a front tracking technique within the MFE formulation.

In one dimension we require to solve (3.37) which may be transformed using (3.36) to give (3.38). We shall seek a piecewise linear MFE solution $V(x, t)$ to the transformed problem (3.38) in the form

$$V(x, t)=\sum a_j\alpha_j. \tag{3.42}$$

Replacing the time derivative in (3.38) with a mobile derivative yields

$$\frac{Dv}{Dt}-v_x\frac{Dx}{Dt}=vv_{xx}+\frac{1}{n}v_x^2. \tag{3.43}$$

At the moving interface $v=0$, assuming v_{xx} remains bounded as $\to 0$, (3.43) reduces to

$$\frac{Dv}{Dt}-v_x\frac{Dx}{Dt}=\frac{1}{n}v_x^2. \tag{3.44}$$

If we denote the position of the interface by $x_I(t)$ and the velocity of this point by $S(x_I(t))$, then by definition

$$\frac{Dv}{Dt}(x_I(t), t)=0$$

and from (3.44) we have

$$S(x_I(t))=-\frac{1}{n}v_x(x_I(t)). \tag{3.45}$$

A similar analysis for the two-dimensional problem

$$v_t=v\nabla^2 v+\frac{1}{n}(\nabla v)^2 \tag{3.46}$$

yields

$$\mathbf{S} = -\frac{1}{n}\nabla v + \mathbf{c} \tag{3.47}$$

at the interface where $\mathbf{c}$ is some arbitrary vector satisfying $\nabla v \cdot \mathbf{c} = 0$.

In one dimension the simplest discrete analog of (3.45) is given by

$$\dot{s}_I = -\frac{1}{n} m_I, \tag{3.48}$$

where $m_I = \Delta a_I / \Delta s_I$ is the gradient of the MFE approximation $V(x, t)$ at the interface node s_I. Numerical experiments show that significantly increased accuracy may be achieved by using

$$\dot{s}_I = -\frac{1}{n}\frac{\partial}{\partial x}(QV(s_I)), \tag{3.49}$$

where $QV(x)$ is a local quadratic fitted to the piecewise linear MFE solution according to

$$QV(s_I) = 0$$
$$QV(s_{I-1}) = a_{I-1}$$
$$QV(s_{I-2}) = a_{I-2}.$$

In two dimensions we approximate ∇v in (3.47) using a simple average of the gradients of the MFE solution $V(x, y, t)$ on elements either side of an interface node. A more detailed description is given in [17, 24].

It may be noted that the transformation $v = u^n$ is the only transformation of the form $v = u^\alpha$ which yields non-zero bounded expressions for the velocity of the moving interface.

In the MFE solution of the transformed problem (3.38) the MFE equations derived by minimising the residual with respect to the velocities of nodes lying on the moving interface are replaced by the discrete approximations to the interface velocity, which act as a constraint on the minimisation. Baines [14] has shown that the MFE matrix remains well-conditioned subject to such constraints and hence fast inversion is still possible using preconditioned conjugate gradients.

For the inner products appearing on the right-hand side of the MFE equations for the solution of (3.38) we again use the quadratic recovery (3.24) for one-dimensional problems and arbitrary smoothing (3.22) in two dimensions. The MFE solution is advanced using explicit Euler time stepping, but a fixed time step is over-restrictive for problems of this type so at each time level t^n we choose an adaptive

time step Δt^n such that the diffusion coefficient V changes by a given percentage θ over each time step, i.e.,

$$\Delta t^n = \left\{ \frac{1}{\max_i \{(\dot{a}_i^n)/(a_i^n)\}} \right\} \times \theta. \tag{3.50}$$

3.3.3. *Numerical Results*

We give numerical results for the MFE solution of the equation

$$u_t = \nabla(u^n \nabla u)$$

in the case of cylindrical symmetry and conservation of total thermal energy (assuming that u represents temperature). A similarity solution exists in this case and is given by

$$u_s(r, t) = \begin{cases} \dfrac{C}{R^2}\left(1 - \left(\dfrac{r}{R}\right)^2\right)^{1/n}, & 0 \leqslant r \leqslant R(t), \\ 0, & r > R(t), \end{cases} \tag{3.51}$$

where the position of the moving front is defined by

$$R(t) = \left[C^n \frac{2}{n} (nq+2)\, t \right]^{1/(nq+2)}$$

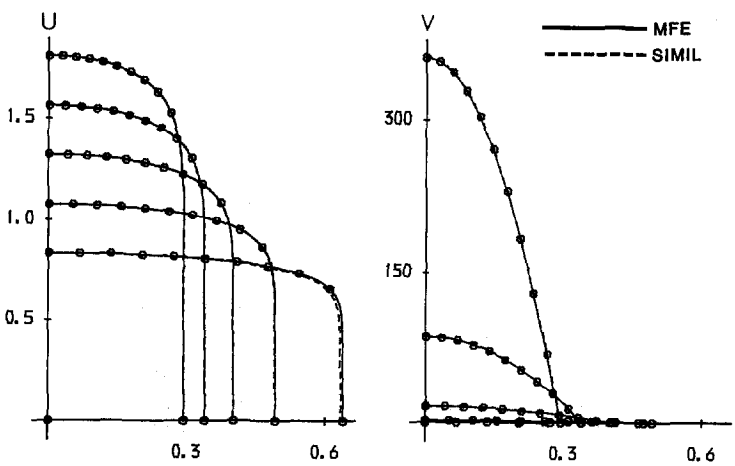

FIG. 3.2. Initial data, MFE (solid line) and similarity (broken line) solutions of one-dimensional non-linear diffusion equation, time $t = 0.0001$ to $t = 1.0$.

with the constant C given by

$$C = \frac{2E}{s(q)}\left(1+\frac{nq}{2}\right)\frac{\Gamma(1/n+q/2)}{\Gamma(1/n)\,\Gamma(q/2)},$$

where E is the constant total thermal energy, q the number of space dimensions, and $s(q)$ the surface area of the unit sphere in q dimensions ($E=1.0$, $q=1, 2$ in the numerical results).

Initial conditions are given by the similarity solution (3.51) for some small starting time $t_s>0$ ($t_s=10^{-4}$ in the results below) and we solve for $x>0$ in one dimension and $x, y>0$ in two dimensions, assuming Neumann conditions on the symmetry boundaries as appropriate. The MFE and similarity solutions for the case $n=10$ in one dimension and $n=5$ in two dimensions are respectively shown in Figs. 3.2 and Figs. 3.3, 3.4a, b.

At each output time the transformation (3.36) is inverted giving the MFE approximation $U(x, t)$ to $u(x, t)$ as

$$U(x, t) = (V(x, t))^{1/n} = (\sum a_j\alpha_j)^{1/n}$$

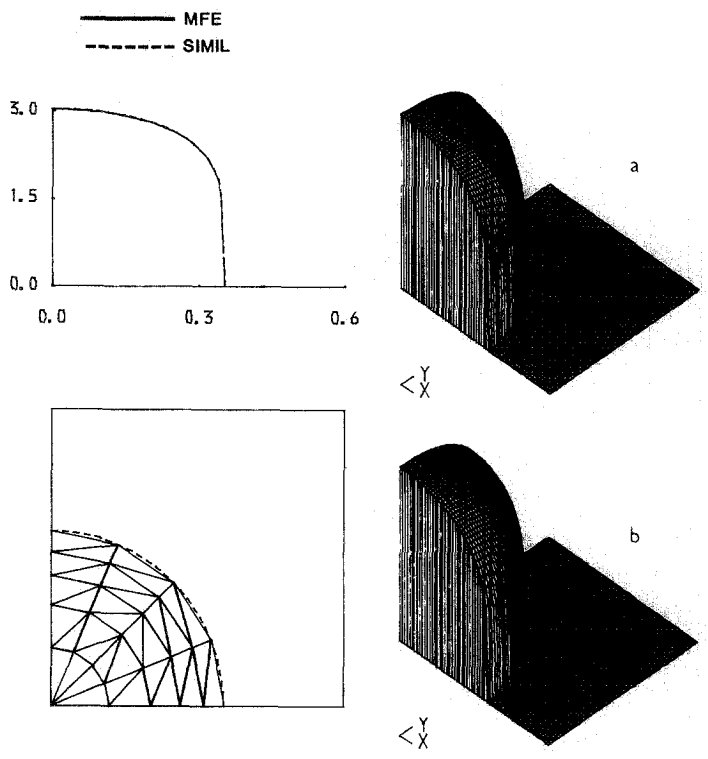

FIG. 3.3. (a) Initial mesh and data for MFE soluttion of two-dimensional non-linear diffusion equation, time $t=0.0001$. (b) Similarity solution.

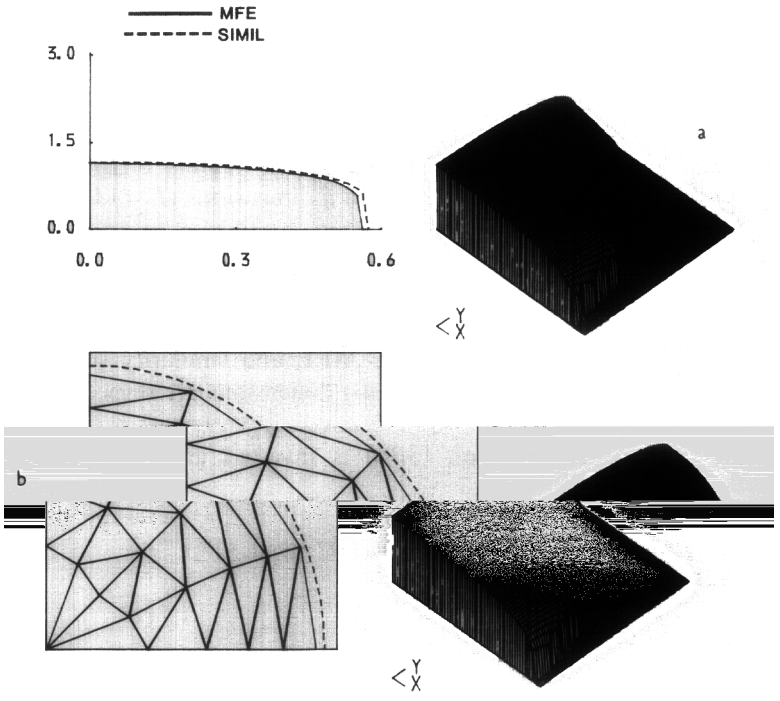

FIG. 3.4. (a) MFE mesh and solution of two-dimensional non-linear diffusion problem, time $t = 0.033$. (b) Similarity solution.

and the solution for U is plotted on a fine mesh between the nodes in the piecewise linear MFE solution for V to give sufficient resolution of the curvature in the solution.

As a further example of the change of variable and front tracking technique we give an MFE solution of the Marshak problem in one dimension (see [25, 17] for details). The Marshak problem is defined by

$$u_t - \tfrac{4}{3} c l_0 (u^{n+3} u_x)_x = 0, \qquad x > 0,\ n > 0 \tag{3.52}$$

subject to the initial and boundary conditions

$$u(0, t) = \tau_0 e^{2\alpha t}$$

and

$$u(x, -\infty) = 0.$$

The values of the arbitrary constants c, l_0, τ_0, and α were chosen as 2.998×10^4, 10, 0.001, and 0.1, respectively, and the initial data was defined using the similarity solution at time $t = 10\ \mu s$. The MFE solutions $U(x, t)$ and $V(x, t)$ for the original

problem (3.52) and the associated transformed problem respectively for the case $n=3$ are given in Fig. 3.5 with outputs at unit intervals of time from $t=25$ to $t=30$ μs.

Finally we show an example using the transformation (3.40) to a problem of type (3.34) which arises in semiconductor process modelling. In this case $D(u)$ in (3.34) is defined by

$$D(u)=\frac{1+\beta n_e}{1+\beta}, \tag{3.53}$$

where

$$n_e=\tfrac{1}{2}(u+\sqrt{u^2+4}).$$

Initial and boundary conditions are given by

$$u(x,0)=\frac{1}{\sqrt{2\pi}\,\sigma_x}\exp(-(x-0.25)^2/2\sigma_x^2)$$

and

$$u_x(0,t)=0 \qquad \text{for all } t>0$$

with the values of the arbitrary constants β and σ_x chosen as 0.05 and 100, respectively.

For the given data, (3.53) is well approximated by

$$D(u)\sim 1+u \tag{3.54}$$

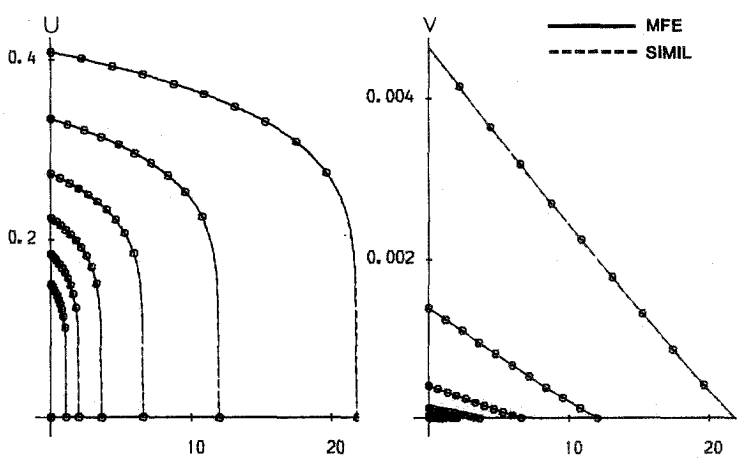

FIG. 3.5. MFE and similarity solutions of one-dimensional Marshak problem time $t=25$ μs to $t=30$ μs.

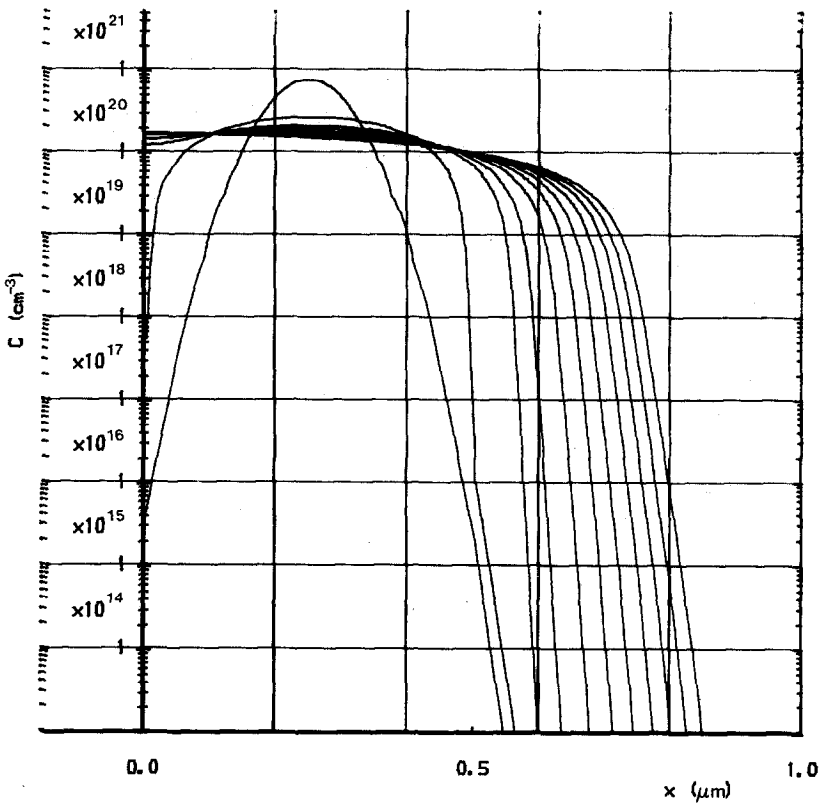

FIG. 3.6. MFE solution of one-dimensional process modelling problem, time $t = 0.0$ to $t = 2000$.

and this approximation is used in (3.40) to define the transformed variable φ as

$$\varphi = u + \ln(u). \tag{3.55}$$

In the transformed problem (3.41) for φ the exact form (3.53) is retained for $D(u)$. We solve the transformed problem using MFE (without front tracking since there is no degeneracy of $D(u)$ here) as for the previous one-dimensional example, and results for the corresponding approximation to the original variable $u(x, t)$ up to time $t = 2000$ are shown in Fig. 3.6 using a logarithmic axis for u.

We move on now to consider systems of hyperbolic equations.

4. SYSTEMS OF EQUATIONS

In this section we give applications of two of the alternative approaches to the MFE solution of a system of evolutionary partial differential equations which are

described in Section 5.4 of Part I. We describe both the use of separate grids for each system component and the use of a common moving grid.

As in Part I we consider the system of equations

$$u_t^{(l)} - L^{(l)}(u^{(1)}, ..., u^{(\mathscr{L})}) = 0, \qquad l = 1, ..., \mathscr{L}, \tag{4.1}$$

and the approximate solutions expressible as finite element expansions

$$U^{(l)} = \sum a_j^{(l)} \alpha_j^{(l)}, \tag{4.2}$$

where $\alpha_j^{(l)}$ are piecewise linear basis functions on a mesh given by the vector of node positions $\mathbf{s}^{(l)}$. In the case of separate grids the $\mathbf{s}^{(l)}$ are independent, while for the single grid case the $\mathbf{s}^{(l)}$ are the same for all l.

When separate grids are employed the MFE method for systems is identical to the scalar method with the exception of the projection of the operator $L^{(l)}(U^{(1)}, ..., U^{(\mathscr{L})})$ (which, in general, depends on all components of the system) into the local space $S_\phi^{(l)}$, i.e., the span of local basis functions $\varphi_{k,\nu}^{(l)}$ on the grid associated with the lth component (see Part I, Section 5.4). In the application presented here the inner products

$$\langle L^{(l)}(U^{(1)}, ..., U^{(\mathscr{L})}), \varphi_{k,\nu}^{(l)} \rangle \tag{4.3}$$

involved in this projection are evaluated using Gaussian quadrature on the elements of the grid represented by the vector of nodal positions $\mathbf{s}^{(l)}$. Note that in one-dimensional problems there is no difficulty in constructing the "global" grid, i.e., the union of all grids, and evaluating the integrals over each sub-element between consecutive nodes. This procedure has no simple multi-dimensional analog, however.

This first computation of this section (Fig. 4.1) shows the approximate solution by this method of a one-dimensional incompressible flow model of three immiscible fluids in a porous medium. The equation system is

$$\begin{aligned} &\frac{\partial u^{(1)}}{\partial t} + \frac{\partial}{\partial x}\left(\frac{(u^{(1)})^2}{(u^{(1)})^2 + (u^{(2)})^2 + (1 - u^{(1)} - u^{(2)})^2}\right) = 0 \\ &\frac{\partial u^{(2)}}{\partial t} + \frac{\partial}{\partial x}\left(\frac{(u^{(2)})^2}{(u^{(1)})^2 + (u^{(2)})^2 + (1 - u^{(1)} - u^{(2)})^2}\right) = 0, \end{aligned} \tag{4.4}$$

where $u^{(1)}$ is the saturation (fraction of total pore space) occupied by the first fluid, $u^{(2)}$ is the saturation of a second fluid and $1 - u^{(1)} - u^{(2)}$ is the saturation of the third fluid. For further details see [13].

When a single grid is used it is easier to evaluate the inner products (4.3), since

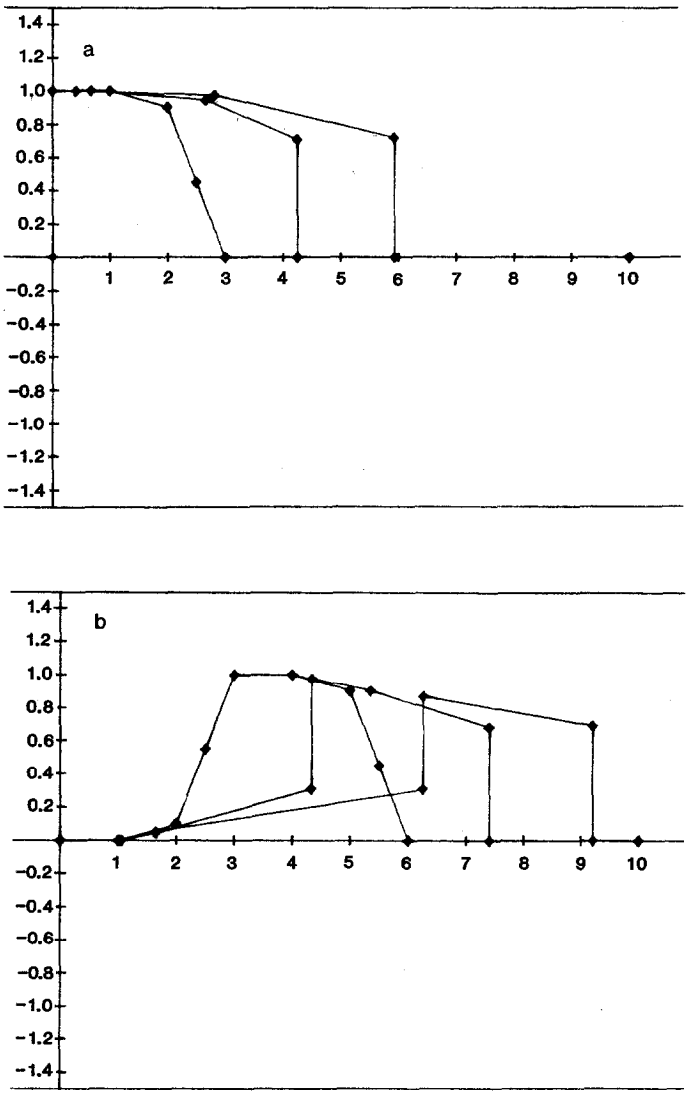

FIG. 4.1. MFE solution of three-phase porous media flow problem, $t = 0.0$ to $t = 3.0$: (a) saturation $u^{(1)}$; (b) saturation $u^{(2)}$.

each component has the same basis functions. However, a particular choice of grid has to be made and the wrong choice can lead to the approximation being unable to reflect the physical situation (see [27]). For this problem we have used separate grids, as described in Section 5.4 of Part I.

The computation shown in Fig. 4.2 is a single grid MFE solution of the standard

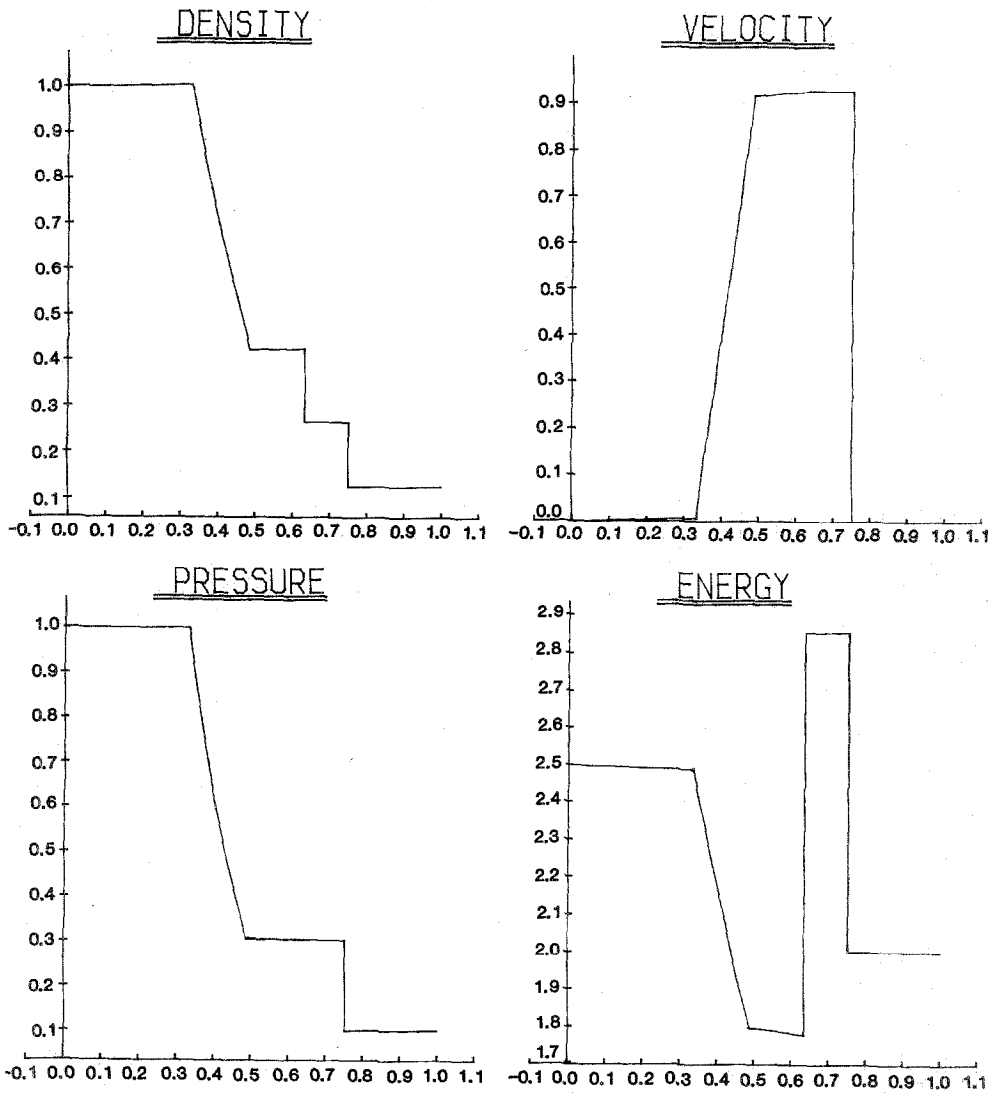

FIG. 4.2. Single grid MFE solution of Sod shock-tube problem, time $t = 0.144$.

shocktube problem as presented by Sod [26]. The equations are the one-dimensional Euler equations of gasdynamics in conservative form, namely,

$$\frac{\partial \rho}{\partial t} + \frac{\partial m}{\partial x} = 0$$

$$\frac{\partial m}{\partial t} + \frac{\partial}{\partial x}\left((\gamma - 1)\, e - \tfrac{1}{2}(\gamma - 3)\, m^2/\rho\right) = 0 \tag{4.5}$$

$$\frac{\partial e}{\partial t} + \frac{\partial}{\partial x}\left((m/\rho)\{\gamma e - \tfrac{1}{2}(\gamma - 1)\, m^2/\rho\}\right) = 0,$$

where ρ, m, e are the density, mementum, and energy and γ is the usual ratio 1.4. The calculation commences at a time $t=0.1$ using initial data from an exact Riemann solver provided by Sweby [28]. (We have not attempted to run the program from $t=0$, since there are insufficient gradients for the method to work on.) Figure 4.2 shows the MFE solution at a time $t=0.144$ using 14 nodes (most of them in the expansion wave). The solution is obtained in a single time step. For further details see [27]. Recent work by Edwards [29] has shown how a modification of the MFE approach using a single grid can lead to a more robust method.

5. Conclusion

In this paper we have exploited the theoretical results of Part I concerning the local nature of the MFE method in one dimension and the good conditioning of the (pre-conditioned) MFE matrix in higher dimensions to construct new efficient solutions of evolutionary partial differential equations which exhibit steep moving fronts. The incorporation of penalty functions has been avoided throughout by the use of a constrained minimisation technique to resolve the problem of parallelism and a time step control to prevent node overtaking. Explicit Euler time stepping is used throughout. A number of hyperbolic test problems, for both scalar equations and systems, have been solved in this way with no addition of artificial viscosity. Shocks are represented as true discontinuities with the shock speed given directly by the Rankine–Hugoniot conditions. For parabolic problems the treatment of second-order operators, both linear and non-linear, has been analysed and a recovery technique introduced which gives improved numerical results and allows an analysis of nodal movement for one-dimensional problems. A change of dependent variable, appropriate for the solution of non-linear diffusion problems, has been used to provide a front tracking technique which can be coupled with the MFE solution procedure.

There remain a number of open questions, particularly regarding the accuracy of the MFE method. When nodes are driven far apart, resolution is lost and insertion of nodes may be needed. It is clear that a monitor of spatial accuracy and resolution is needed for this purpose and one suggestion is the residual of the differential equation itself. We have not used such a monitor in the examples given here. Time steps are guided by considerations of node overtaking or by percentage variations of a physical quantity such as the diffusion coefficient. Stability is lost when nodes overtake and this appears to be a counterpart to oscillations in the FFE method. There is also still scope for some practical error analysis and it is hoped that the simplicity of the approach adopted here may help to stimulate such an analysis.

ACKNOWLEDGMENTS

We thank Professor K. W. Morton of Oxford University for many useful discussions and Robin Dixon and Mike Edwards of Reading University for help in producing the results given here. One of us (IWJ) acknowledges the financial assistance of the Science and Engineering Research Council through a CASE studentship with AWRE.

REFERENCES

1. M. J. BAINES AND A. J. WATHEN, *J. Comput. Phys.* **78**, (1988).
2. K. MILLER AND R. N. MILLER, *SIAM J. Num. Anal.* **18**, 1019 (1981); K. MILLER, *SIAM J. Num. Anal.* **19**, 1033 (1981).
3. R. GELINAS, S. K. DOSS, AND K. MILLER, *J. Comput. Phys.* **10**, 202 (1981).
4. J. K. DUKOWICZ, *J. Comput. Phys.* **56**, 324 (1984).
5. M. C. MOSHER, *J. Comput. Phys.* **57**, 157 (1984).
6. A. N. HRYMAK, G. J. MCRAE, AND A. W. WESTERBERG, *J. Comput. Phys.* **63**, 168 (1986).
7. A. J. WATHEN, *SIAM J. Num. Anal.* **23**, No. 4, 797 (1986).
8. A. J. WATHEN AND M. J. BAINES, *IMA J. Num. Anal.* **5**, 161 (1985).
9. T. DUPONT, *Math. Comput.* **39**, 85 (1982).
10. C. P. PLEASE, University of Reading, U.K., private communication (1986).
11. P. K. SWEBY, University of Reading, U.K., private communication 1986).
12. P. CONCUS AND W. PROSKUROWSKI, *J. Comput. Phys.* **30**, 153 (1979).
13. A. J. WATHEN, Ph.D. thesis, University of Reading, U.K., 1984 (unpublished).
14. M. J. BAINES, Numerical Analysis Report 15/85, University of Reading, U.K., 1985 (unpublished).
15. A. C. MUELLER AND G. F. CAREY, *Int. J. Numer. Methods Eng.* **21**, 2099 (1985),
16. K. W. MORTON, University of Reading, U.K., private communication (1982).
17. I. W. JOHNSON, Ph.D. thesis, University of Reading, U.K., 1986 (unpublished).
18. W. F. AMES, *Nonlinear Partial Differential Equations in Engineering* (Academic Press, New York, 1965).
19. A. B. TAYLER, J. B. OCKENDON, AND A. A. LACEY, *SIAM J. Appl. Math.* **42**, 1252 (1982).
20. Y. A. B. ZEL'DOVICH AND A. S. KOMPANEETS, *Izv. Akad. Nauk. SSSR* (1950).
21. K. TOMOEDA AND M. MIMURA, *Hiroshima Math. J.* **13**, 273 (1983).
22. P. MEEK AND J. NORBURY, *SIAM J. Num. Anal.* **21**, 883 (1984).
23. C. P. PLEASE AND P. K. SWEBY, Numerical Analysis Report 5/86, University of Reading, U.K., 1986 (unpublished).
24. I. W. JOHNSON, Numerical Analysis Report 12/85, University of Reading, U.K., 1985 (unpublished).
25. R. MARSHAK, *Phys. Fluids* **1**, 1 (1985).
26. G. SOD, *J. Comput. Phys.* **27**, 1 (1978).
27. M. J. BAINES AND A. J. WATHEN, *Appl. Num. Math.* **2**, 495 (1986).
28. P. K. SWEBY, University of Reading, U.K., private communication (1986).
29. M. G. EDWARDS, Numerical Analysis Report 20/85, University of Reading, U.K., 1985 (unpublished).
30. K. MILLER, in *Accuracy Estimates and Adaptive Refinements in Finite Element Computations*, edited by I. Babuška, O. C. Zienkiewicz, J. Gago, and E. R. de A. Oliveira (Wiley, New York, 1986), p. 325.